



T. Adeyelu et al. / Neuroscience 548 (2024) 50-68

# VTA Excitatory Neurons Control Reward-driven Behavior by Modulating Infralimbic Cortical Firing

Tolulope Adeyelu, a Tashonda Vaughn b and Olalekan M. Ogundele a,\*

Abstract—The functional dichotomy of anatomical regions of the medial prefrontal cortex (mPFC) has been tested with greater certainty in punishment-driven tasks, and less so in reward-oriented paradigms. In the infralimbic cortex (IL), known for behavioral suppression (STOP), tasks linked with reward or punishment are encoded through firing rate decrease or increase, respectively. Although the ventral tegmental area (VTA) is the brain region governing reward/aversion learning, the link between its excitatory neuron population and IL encoding of reward-linked behavioral expression is unclear. Here, we present evidence that IL ensembles use a population-based mechanism involving broad inhibition of principal cells at intervals when reward is presented or expected. The IL encoding mechanism was consistent across multiple sessions with randomized rewarded target sites. Most IL neurons exhibit FR (Firing Rate) suppression during reward acquisition intervals (T1), and subsequent exploration of previously rewarded targets when the reward is omitted (T2). Furthermore, FR suppression in putative IL ensembles persisted for intervals that followed reward-linked target events. Pairing VTA glutamate inhibition with reward acquisition events reduced the weight of reward-target association expressed as a lower affinity for previously rewarded targets. For these intervals, fewer IL neurons per mouse trial showed FR decrease and were accompanied by an increase in the percentage of units with no change in FR. Together, we conclude that VTA glutamate neurons are likely involved in establishing IL inhibition states that encode reward acquisition, and subsequent reward-target association. © 2024 IBRO. Published by Elsevier Inc. All rights reserved.

Key words: VTA, mPFC, pyramidal cells, firing rate, reward.

#### INTRODUCTION

The medial prefrontal cortex (mPFC) is a neocortical region that governs executive behavior, learning, memory, and guided decision-making, among other functions (Ferenczi et al., 2016; Nakayama et al., 2018; Coley et al., 2021; Hardung et al., 2021). The population of neurons in the prefrontal cortex is heterogeneous. In addition to the anatomical neuronal heterogeneity, parts of the prefrontal cortex can also be distinguished functionally (Hoover and Vertes, 2007; Nakayama et al., 2018; Shipman et al., 2018; Capuzzo and Floresco, 2020; Anastasiades and Carter, 2021; Green and Bouton, 2021). Notably, the cingulate gyrus (CG), infralimbic (IL), and prelimbic (PrL) cortical regions contribute to different behavioral responses through local cortical, and

extra-cortical pathways (Euston et al., 2012; Oler and Fudge, 2019; Chen et al., 2021). Among other functions, the mPFC is central to novelty and context discrimination neural circuits that guide the brain to focus on what is new, and relevant to a particular situation in time (Schwartz et al., 2002; Nett and LaLumiere, 2021). Through this mechanism, the brain associates environmental stimuli with events and recalls these associations to guide future decisions (van Kesteren et al., 2012; Park et al., 2021; Wang et al., 2021; Wu et al., 2022). These adaptive mechanisms are pertinent to survival, and the ability to learn or recall what is learned towards obtaining rewards or avoiding punishments.

There is consensus that mPFC principal neurons are dichotomous such that the PrL neurons promote behavioral expression (i.e., GO), and infralimbic neurons suppress behavioral expression (i.e., STOP). Together, the overarching functional dichotomy of the mPFC depicted as "PrL-GO/IL-STOP" has been tested with greater certainty in punishment-oriented tasks, and to a lesser extent in reward-driven tasks (Moorman and

E-mail address: ogundele@lsu.edu (O. M. Ogundele). Abbreviations: CG, cingulate gyrus; FR, firing rate; IL, infralimbic; IL, infralimbic cortex; mPFC, medial prefrontal cortex; PrL, prelimbic; VTA, ventral tegmental area.

<sup>&</sup>lt;sup>a</sup> Department of Comparative Biomedical Sciences, Louisiana State University School of Veterinary Medicine, Baton Rouge, LA 70803, United States

<sup>&</sup>lt;sup>b</sup> Department of Environmental Toxicology, College of Agriculture, Southern University A&M College, Baton Rouge, LA 70813, United States

<sup>\*</sup>Corresponding author.

Aston-Jones, 2015; Moorman et al., 2015; Riaz et al., 2019; Capuzzo and Floresco, 2020; Nett and LaLumiere, 2021). A prevailing school of thought proposes that the firing rate (spikes/sec) of PrL principal neurons increases in reward-oriented tasks while the FR of IL principal neurons is mostly suppressed in similar tasks (Ishikawa et al., 2008; Moorman and Aston-Jones, 2015; Moorman et al., 2015). Therefore, either exogenous stimulation of IL neurons or the inhibition of PrL neurons can suppress the expression of reward-oriented behavior (Jonkman et al., 2009; Moorman and Aston-Jones, 2015; Nett and LaLumiere, 2021).

Results of recent studies provide evidence that the "PrL-GO" or "IL-STOP" component of the mPFC functional dichotomy is not "all or none". Rather, subpopulations of principal neurons in ensembles tune the directionality of their firing rate (ΔFR) depending on the valence of the context or task (Ishikawa et al., 2008; Moorman and Aston-Jones, 2015). Thus, it is likely that various sunsets of principal cells in an ensemble will exhibit an increase, a decrease, or no change in  $\Delta$ FR directionality if a reward is presented, omitted, or paired with a probability of punishment (Moorman and Aston-Jones, 2015; Ferenczi et al., 2016; Park and Moghaddam, 2017; Jacobs and Moghaddam, 2020; Chen et al., 2021; Green and Bouton, 2021). Although inhibition of IL principal cell firing is pertinent to the expression of rewardoriented behaviors, the extent of such inhibition within IL ensembles when a reward is present, compared to when it is anticipated but not presented remains unclear. Furthermore, it is unclear whether the suppression of IL firing states that encode reward-oriented events are similar in threshold and timing when the location or context associated with the reward is randomized per session, and over a prolonged duration.

In addition to the suppression of IL firing rate, the expression of reward-oriented behavior is also dependent on the activation state of neuron subgroups in the mesocorticolimbic ventral tegmental area (VTA) (Chau et al., 2004; Lisman and Grace, 2005; Luscher and Malenka, 2011; Salvetti et al., 2014; Broussard et al., 2016; Hu, 2016; Bouarab et al., 2019). There is significant evidence that modulation of the VTA impacts cortical decision-making (Lisman and Grace, 2005; Brischoux et al., 2009; Ghanbarian and Motamedi, 2013; McNamara et al., 2014; Funahashi, 2017; Duszkiewicz et al., 2019). Recent studies also demonstrate that reciprocal connections between the VTA and mPFC moderate broad aspects of behavioral response to contextual valence (Moorman et al., 2015: Park and Moghaddam, 2017). Although the VTA contains mostly dopamine neurons, its projections to the mPFC also include glutamate and GABA tracts that exert modulatory effects on the firing properties of principal neurons to drive diverse behavioral responses (Floresco et al., 2001; Ford and Williams, 2008; Lammel et al., 2014; Hu, 2016; Ntamati and Luscher, 2016; Yoo et al., 2016; Bouarab et al., 2019; Liu and Kaeser, 2019). Specifically, VTA glutamate neurons are responsive to both punishment and rewardoriented executive tasks and exert modulatory effects

on excitatory and inhibitory neuron populations in the IL (Yoo et al., 2016; Montardy et al., 2019).

The directionality of  $\Delta FR$  for subsets of IL principal cells, and the timing of activation or suppression is pertinent for behavioral response (Moorman and Aston-Jones, 2015; Moorman et al., 2015; Park and Moghaddam, 2017; Nett and LaLumiere, 2021). Although anatomical evidence demonstrates VTA glutamate innervation in the various anatomical regions of the mPFC (Yoo et al., 2016; Park and Moghaddam, 2017; Montardy et al., 2019), it remains unclear how VTA glutamate inputs modulate the timing and directionality of IL principal cell ensembles duing reweard-oriented tasks. Here, we combined in vivo IL recording with optogenetic inhibition of VTA glutamate neurons in freely behaving mice during food reward acquisition in a random location (trial 1), followed by an omission of the reward at the same location (trial 2). Our results show the majority of principal neurons in IL ensembles exhibit FR suppression at intervals of reward acquisition, or exploration of a previously rewarded target without a reward present. For multiple experimental sessions, with randomized target locations, the observed IL encoding pattern was consistent. However, pairing the reward with VTA glutamate inhibition reduced the fidelity of FR suppression in IL ensembles, leading to a decrease in reward-driven behavioral expression.

#### **EXPERIMENTAL PROCEDURES**

The IACUC committee of the LSU School of Veterinary Medicine approved all procedures involving the handling and use of animals. Adult male Vglut2<sup>Cre</sup> mice were weighing  $\sim\!25$  g used for this study (n=4). Mice were anesthetized by intraperitoneal ketamine/xylazine (100:10 mg/kg) injection. After the plane of anesthesia was established, the head was fixed on a stereotaxic frame to expose the cranial sutures. Anteroposterior (AP) and mediolateral (ML) coordinates of the infralimbic cortex (AP: +1.94 mm, ML: +0.3 mm) and VTA (AP: -3.08 mm, ML: +0.5 mm) were determined relative to the bregma, and craniotomies were performed over these regions.

#### Electrode implant in the mPFC

Chronically implantable silicon probes (Neuronexus, USA) were lowered into the mPFC such that the four electrode contact sites were positioned in the infralimbic cortex (Fig. 1(A)). Stainless steel ground and reference wires on the probes were connected to screws fixed in the occipital bone. The neural probe was connected to a preamplifier head stage and tethered to an amplifier controller (Intantech, USA) to detect spontaneous neural activity in the layers of the cortex. Multiunit spikes were detected by using a lower—upper frequency cutoff range of 0.3–5 kHz, and a sampling rate of 25 K/s. The position of the electrode contact sites was adjusted to dorsoventral coordinates (DV: 3.2 mm) that correspond to the infralimbic cortex (Fig. 1(B)).

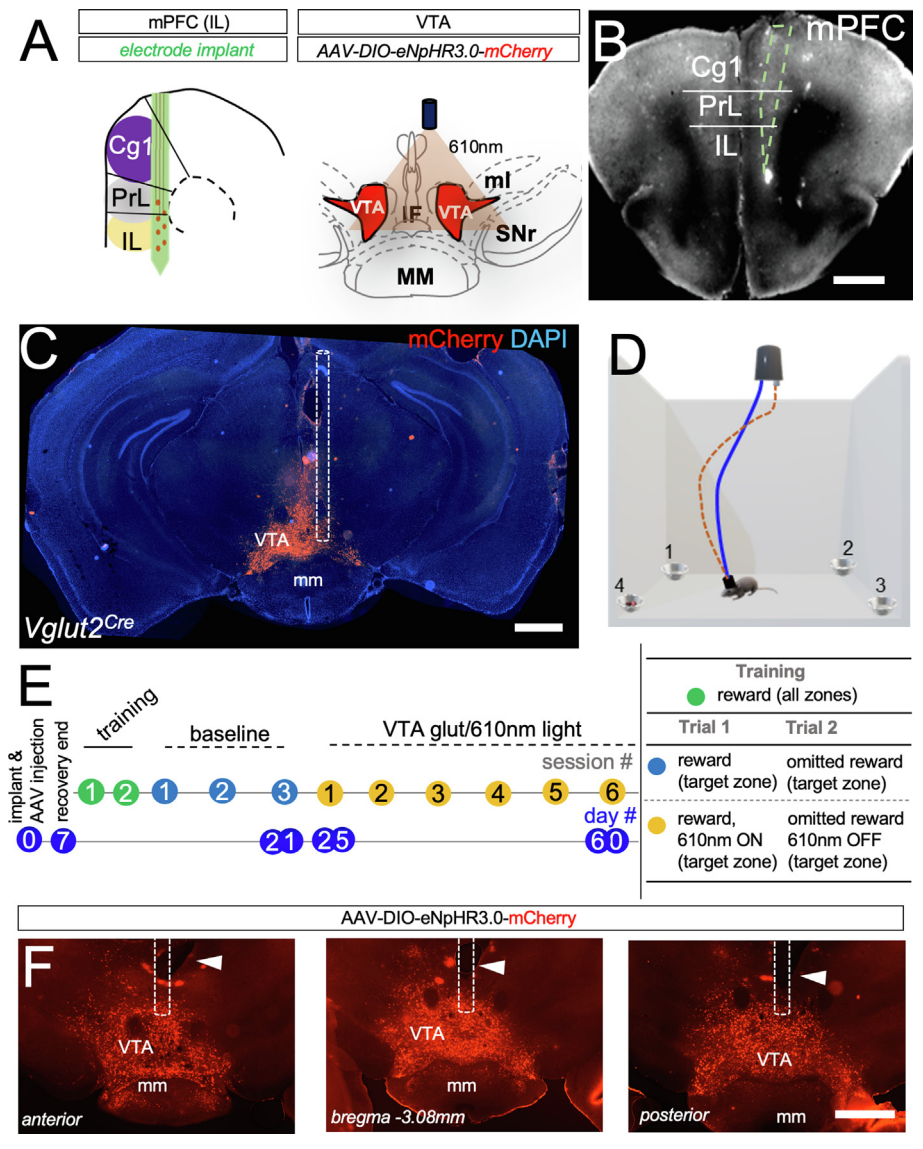


Fig. 1. Optogenetic modulation of VTA glutamate neurons and infralimbic cortical (IL) recording in a reward-driven task. (A) Schematic illustration of electrode placement in the IL and double floxed AAV-DIO-eNpHR3.0-mCherry expression in VTA glutamate neurons of  $Vglut2^{Cre}$  mice. Fiber optic cannula placement in the VTA demonstrates 610 nm light radius (20 Hz) applied for VTA modulation (bregma -3.08 mm AP. VTA: ventral tegmental area, MM: mammillary nucleus, SNr: substantia nigra reticular part, IF: Interfascicular nucleus, mI: medial lemniscus). (B) A representative brain slice showing the track of an implanted silicon neural probe shank in the IL (scale bar = 1 mm). (C) Fluorescence image showing the expression of AAV-DIO-eNpHR3.0-mCherry in VTA glutamate neurons of  $Vglut2^{Cre}$  mice (scale bar = 1 mm). (D) Schematic illustration of the experimental setup for reward-oriented exploration behavioral task. (E) Schematic illustration of experimental timeline post-surgery illustrating baseline experiments (days 7–21) and VTA modulation (days 25–60). Table illustration of training, baseline, and VTA modulation sessions. (F). Representative fluorescence image demonstrating the spread of AAV-DIO-eNpHR3.0-mCherry in the VTA of a  $Vglut2^{Cre}$  mouse (scale bar = 0.75 mm).

### AAV injection and fiberoptic cannula placement in the VTA

Double floxed adeno-associated virus (AAV5-DIO-eNpHR3.0-mCherry) harboring light-controlled inhibitory opsin (eNpHR3.0) (AddGene, USA) was injected into the VTA of Vglut2<sup>Cre</sup> mice at a depth (DV) of 4.4–4.5 mm. The AAV was delivered at 60~nl per minute, and up to a volume of 600~nl was injected into the VTA close to the midline (ML = 0.3–0.5~mm) to facilitate bilateral

expression of eNpHR3.0 and mCherry (Fig. 1(C)). The injection needle was in place for 15 min before the gradual withdrawal. Subsequently, a fiberoptic cannula (250 µm thick) was positioned in the AAV injection site within the medial VTA (Fig. 1(C)) up to a depth of 4.30-4.35 mm. Adequate in-operative and post-operative care was given to mitigate pain and discomfort that may result from the procedure. Animals recovered before 72 h and were assessed in behavioral tests after 7 days.

## Food reward acquisition and VTA photomodulation

The same set of mice was assessed in three baseline and six optogenetic modulation sessions. All behavioral test sessions were acquired with Ethovision XT15 fitted with a hardware control module for timelocking behavioral events with neural recording and optogenetic modulation. Mice with neural implants were familiarized with a rectangular open-field chamber containing four reward pots, each positioned in a corner, and numbered clockwise (i.e., 1-4, Fig. 1(D)). For the training session, food was presented at all locations so that mice associate each pot with a reward, and were motivated to explore in search of food after a fasting period (3-4 h). The training session was performed at 48 h and 24 h before the experimental test session.

The experimental session assessed the affinity of a mouse for a single rewarded target compared to three non-rewarded (non-target) sites. As such, when a mouse explores the target to obtain the food reward (reward, *Trial 1*: 10 min), the duration spent exploring the target, and the frequency of revisits to the target were compared to the non-target outcomes. After a

45-minute waiting period in the home cage, the animal was re-assessed for its affinity for the target site without a reward present (omission, *Trial 2*: 10 min). Similarly, time spent exploring the target (without a reward), and the frequency of revisits to the target were compared to the non-target outcomes for the omission trial (T2).

In the first trial, it is expected that the mouse will obtain the food reward from the target position, explore the nonreward cups (non-target positions), and return more frequently to the reward target for the duration of the trial (Figure 1D, e.g., position 4). This will indicate that the mouse recognized the target location for the trial, and has associated the location with the reward. Similarly, during the omission trial, it is expected that the mouse will visit the target position (i.e., position 4) more frequently than non-target positions in anticipation of a reward since this site is now associated with the reward received during the first trial. For each trial and session, the expression of foraging behavior was assessed by the mean distance and velocity. The percentage of correct attempts or errors was also compared for the rewarded trial (T1) and omission trials (T2). A correct attempt represents a visit to the target from any nontarget position. Conversely, error in an attempt represents transitions from one non-target to another.

Across sessions, the target position was randomized such that none was repeated in sequence. Here, "reward acquisition (T1)" or "previously rewarded exploration (T2)" involves nose point positioning over the target for more than 1 s. For the three baseline sessions (no VTA modulation in T1), positions 3, 1, and 4 were selected as targets, and in sequence. These sessions were performed from post-surgery day 7 to 21 (Fig. 1(E)). Acquiring a reward from the target (T1), and exploring a previously rewarded target (T2) was mapped via a TTL output signal synchronized with the continuously recorded infralimbic cortical spikes. For these trials, non-target sites were mapped to a second TTL output and time-locked with the continuously sampled spikes. Since robust AAV expression is expected from 21 days post-injection, six experimental sessions with paired reward and VTA glutamate inhibition were performed between day 25 to day 60 (Fig. 1(E)). To synchronize events, a TTL signal driven by reward acquisition (T1) was split to trigger 20 Hz pulses from 610 nm LED when the nose point is in a target zone (pot) for more than 1 s. In subsequent omission trials, the 610 nm light was turned OFF. The location of the fiberoptic cannula in the VTA was verified by fluorescence localization of VTA glutamate neurons, and tissue lesions above the VTA (Fig. 1(F)).

Spike sorting and single unit detection: In an Offline spike sorter (OFSS, Plexon, USA), extracellular spikes were pre-processed with a Butterworth filter (300 Hz to 5,000 Hz) to remove anatomical drifts and local field potential artifacts. Single unit clustering of the recorded spike was performed by principal component analysis (PCA) to detect putative mPFC principal neurons. To improve the signal-to-noise ratio, an amplitude discrimination step was implemented in the OFSS. A lower peak crossing threshold that is 5x the root mean square (RMS) was set for each electrode channel to eliminate noise and artifact spikes (Quiroga, 2012; Chung et al., 2017; Swindale et al., 2017). Where necessary unsorted spikes were manually invalidated, since more than one putative unit was detected on each electrode channel, and spikes were further discriminated against based on the interspike interval (ISI). As such, for two spikes to be assigned to the same putative unit, the ISI must be > 1 ms. This step accounts for the refractory period in action potential and prevents ISI violation

(Quiroga, 2012; Chung et al., 2017). Post-processing overlap analysis (splitting and merging) was performed in the Spikesorter software (Swindale et al., 2017).

Characterizing cortical PYR units in ensembles: Waveforms of clustered units were inspected across all channels. Viable units were accepted based on the autocorrelogram (ACG), firing rate (FR Hz), and waveform valley-to-peak time (u sec). Putative units with a valley-to-peak time range of 400- $650~\mu s$  and distinct ACG peaks at 0 ms, followed by a rapid decay (50 ms) were characterized as putative pyramidal cells (Bartho et al., 2004; Sotres-Bayon et al., 2012). Interneuron ACGs have a distinct trough at 0 ms, with sustained activity. Interneurons were further distinquished from pyramidal cells by the absence of complex spiking and higher firing rate scores. Putative units identified as cortical principal cells have a mean firing rate that ranges between 0.1 to 5 Hz. Based on the shape of the waveform, ACG, and firing rate, it is likely that most of these neurons are glutamatergic cells (Bartho et al., 2004; Moorman and Aston-Jones, 2015).

Statistics: Sorted spikes for detected putative principal cells were exported to Neuroexplorer (Nex Technologies, USA) for further analysis of the FR, and comparison of the change in FR across intervals. Results from spike analysis and Ethovision XT15 behavioral tracking were further analyzed in OriginPro 2024 software. The same group of four mice underwent three baseline sessions (day 7-21 post-surgery) and six VTA modulation sessions (day 25-60 post-surgery). all experimental sessions, synchronized behavioral tests and IL firing rate outcomes were compared for T1 (target containing reward) and T2 (reward omitted at target). Normality distribution was determined using Kolmogorov-Smirnov test. With normally distributed data, a paired T-test was conducted to determine if mice exhibited similar affinity for the target when it was rewarded (T1), and after 45 min when it was simply associated with a reward (T2: omission). In subsequent analysis, the outcomes for each mouse/trial/session were compared between baseline and VTA modulation sessions using a Twosample T-test to determine the significance when equal variance is assumed or not assumed. By comparing T1 in baseline sessions with those photomodulation sessions, the group (i.e., mice) served as its control in testing the effect of VTA glutamate neurons on reward-linked behavior and IL firing patterns.

One-way ANOVA – with Tukey post hoc test and F-value of variance – analysis was used to compare all baseline and VTA modulation trials (T1: rew, T2: o-rew, T1: rew/VTA glu 610 nm ON, and T2:o-rew/610 nm OFF). Specifically, mean distance (cm) and mean velocity (cm/s) were compared to detect changes in chamber exploration propensity. Likewise, the mean spontaneous FR (Hz) was compared to detect any variation in IL principal cell activity during exploration events not associated with target or non-target intervals.

Statistical analysis for IL firing rate measures was presented in two forms. First, firing rate outcomes were determined for neurons sampled during a specific trial

(T1 or T2) across all experimental sessions. Secondly, the outcomes were presented as averages of IL firing rate per mouse for each trial/session. The results for both forms of analysis were comparable.

#### **RESULTS**

# Behavioral test outcome for reward-oriented exploratory behavior

For this test, mice performed a task to associate a specific location - one out of four - with a food reward. The sessions were conducted every three days, and the food reward was randomized across all the sessions. During each session, mice were presented with a set of four locations (pots), with one location containing the reward in the trial (T1: "rewarded target"), and the same location being without a reward in the second trial (T2: "previously rewarded target"). The remaining three locations were considered "non-targets" because they did not contain a reward in T1 and were not associated with a reward in T2. Mice were expected to show a preference for the target location when the reward was presented (T1). After 45 min, it is expected that mice will preferentially explore the previoulsy rewarded target location in anticipation of a reward when it was omitted (T2). This behavior would indicate that mice associated the location - during T2 - with the previously obtained food reward in T1. By allowing several days between sessions, the novelty of the task was maintained. Additionally, randomizing the target location ensured that each learning session was unique and avoided repetition in the target sequence across sessions.

During baseline sessions, mice explored reward pots and obtained a reward from the target in T1. Overall, mice showed a preference for the rewarded target in comparison to non-targets and revisited the target multiple times during T1 (Movie 1). A representative activity tracking (heat) map for a subject mouse in Movie 1 (Fig. 2(A)) further demonstrated this. In omission trials, mice preferred the previously rewarded target position over the non-targets (Trial 2; Movie 2). These observations remained consistent across experimental sessions with different (randomized) target positions

Movie 1.



#### Movie 2.



The results showed that mice exhibit a strong affinity for the "target location" in T2 once it has been associated with a previous reward (during T1). The mean distance covered (Fig. 2(**B**), p = 0.47) and velocity of chamber exploration (Fig. 2(C), p = 0.28) were not significantly different between the reward acquisition (T1) and subsequent omission (T2) trials. Additionally, the frequency of visits to the target position (Fig. 2(**D**), p = 0.56) and exploration duration in the target zone (Fig. 2(E), p = 0.96) were also similar for the reward acquisition and omission trials. The frequency of direct target re-visits (Fig. 2(F), p = 0.14) and non-target revisits (Fig. 2(G), p = 0.69) also did not change significantly when rewarded trials were compared with the subsequent omission trials. Lastly, the percentage of correct attempts (Fig. 2(H), p = 0.23) and errors (Fig. 2(1), p = 0.13) were comparable between the two trials. Overall, the results showed that mice were able to identify and locate a reward at random locations, and continued to search for it at the same location even when it was omitted subsequently.

## VTA glutamate neurons in reward learning and context association

The role of VTA glutamate neurons in reward-oriented exploratory behavior and context association was studied by selectively inhibiting the neurons with 610 nm light pulses when the animal reached the target cup to acquire the food reward (T1-reward/610 nm ON). The photoinhibition did not affect the chamber exploration behavior across experimental trials and sessions. Therefore, there was no significant difference in the mean distance (Fig. 3(A), p > 0.05. ANOVA  $F_{value} = 0.6344$ , DF = 3, and p = 0.596) or velocity (Fig. 3(B), p > 0.05. ANOVA  $F_{value} = 2.547$ , DF = 3, and p = 0.065) recorded during reward acquisition (T1) and omission (T2) trials of baseline and VTA modulation sessions.

Although chamber exploration was unaffected, selective inhibition of VTA glutamate neurons reduced the interest of mice in the food reward (Fig. 3(C), reward). As a result, VTA glutamate inhibition caused a decrease in the frequency of visits to the rewarded target in T1 (T1-reward/610 nm; **Movie 3**). In the subsequent omission trial,

for which VTA glutamate inhibition is removed (610 nm light is turned OFF), mice did not show a preference for the previously rewarded target position that was paired with VTA glutamate inhibition (T2-omission/610 nm OFF; **Movie 4**). The results show that inhibiting VTA glutamate neurons during reward acquisition decreases the frequency of reward target visits (Fig. 3(**D**), p = 0.03) and the duration of exploration (Fig. 3(**E**), p = 0.02) in the omission trial. In comparison, the frequency and exploration duration during baseline reward acquisition and omission were not significantly different (Fig. 2(**D-E**)).

Movie 3.



Movie 4.



During reward acquisition trials (T1), if the VTA glutamate neurons are selectively inhibited (610nm ON), the frequency of target revisits during omission trials decreases significantly (Fig. 3( $\mathbf{F}$ ), p=0.002). However, the frequency of revisits to non-target positions does not change significantly (Fig. 3( $\mathbf{G}$ ), p=0.13). This implies that inhibition of VTA glutamate neurons during reward acquisition had no significant effect on chamber exploration but reduced the affinity of mice for the target when the reward was omitted. As a result, in omission trials (T2), the percentage of correct events that indicate

transitions from non-targets to a previously rewarded target, decreased when the prior reward acquisition event (T1) was paired with VTA glutamate inhibition (Fig. 3(H), p=0.0498). There is also an increase in errors, indicating that mice recorded an increase in transition between multiple non-targets (Fig. 3(I), p=0.008). These results show that pairing reward acquisition with VTA glutamate neuron inhibition decreased the weight of reward events that are attributed to the target.

## Change in FR of putative mPFC cells encodes reward-oriented exploratory behavior

IL cortical neural spikes were sampled continuously and specific intervals spent at target and non-target locations were determined using TTL outputs. When a mouse gets a reward (T1) or explores a previously rewarded target cup (T2) TTL signals are generated if the nose point exceeds 1 s inside the target zone (i.e., the reward cup). TTL signals connoting specific behavioral events time-locked target and non-target intervals with the IL spike train (baseline), or IL spike train with photo inhibition (VTA modulation). Putative IL neurons, which appear mostly glutamatergic, were identified by the shape of waveforms, firing rate, and autocorrelogram (ACG) (Fig. 4(A)) (Bartho et al., 2004; Moorman and Aston-Jones, 2015; Zielinski et al., 2019). Clusters of mPFC principal neurons used for subsequent analysis were selected based on waveform valley-to-peak duration and FR (Fig. 4(B)). Putative IL neurons with a minimum FR of 0.2 Hz and a maximum range of 5 Hz, having narrow or wide waveforms were included for analysis. The FR of putative IL units during target intervals was normalized with the respective spontaneous FR values derived from the same spike train.

# IL representation of reward acquisition, and subsequent omission at a target

Across three separate baseline sessions (Fig. 2(A-I)), mice acquired the food reward (T1) and showed a comparable preference for the target when the reward was removed subsequently (T2) (Fig. 5(B)). Thus, there was no significant difference in the target index (targ./(targ. + non-targ.) for mice during the reward and omission trials. This result suggests that mice with normal foraging behavior have a similar preference for a target when it contains or is associated with a reward (Fig. 5(C),  $\rho = 0.13$ ).

Spikes of putative IL principal neurons sampled during the reward acquisition intervals (T1) and subsequent exploration of a previously rewarded target (T2) are depicted as raster trains. Multi-unit rasters show the spike response of putative principal cell units in IL ensembles (Cell #) before, during, and after the tracked nose point is above the center of a target. Multi-unit rasters recorded from a mouse IL during reward acquisition intervals (T1) and subsequent intervals

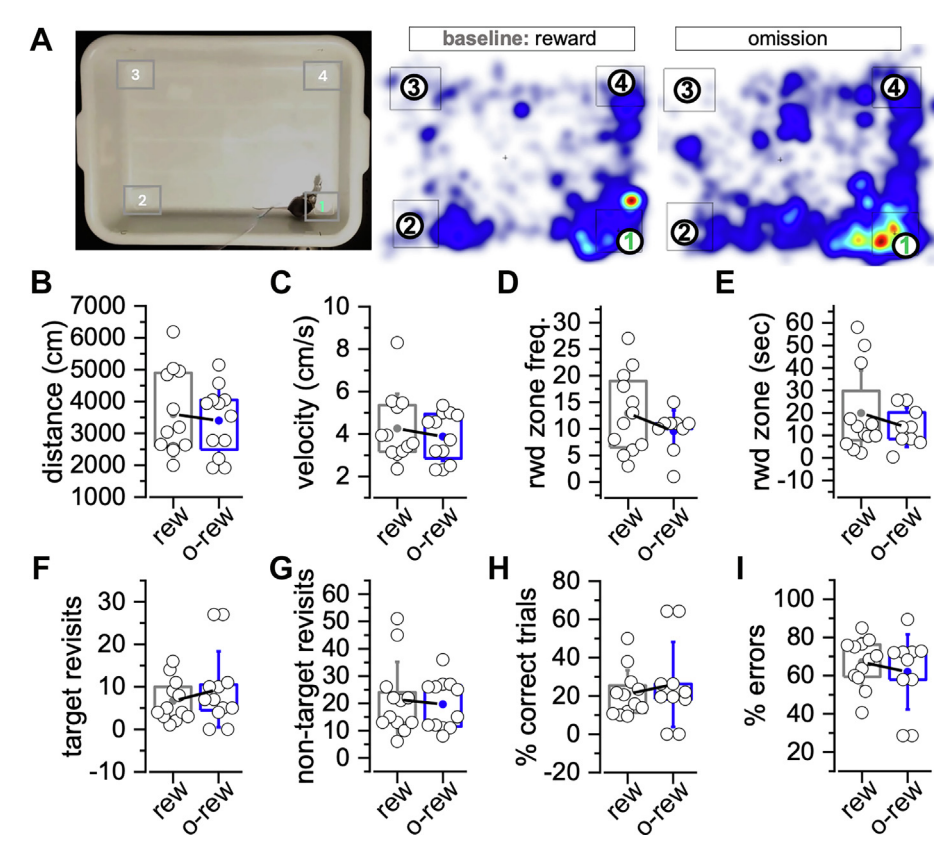


**Fig. 2. Baseline reward-oriented exploratory behavior. (A)** Sample heatmap that depicts the exploration activity of a mouse when a reward is presented and omitted subsequently at target position 1. Paired T-test comparison (graphs) of behavioral task performance during reward acquisition and subsequent omission was not significant: **(B)** Distance (p = 0.47, ns). **(C)** Velocity (p = 0.28, ns). **(D)** Frequency of visits to the reward target position (p = 0.56, ns). **(E)** Total duration at the reward target position (p = 0.96). **(F)** Total number of reward or arget position visits (p = 0.14, ns). **(G)** Total number of visits to non-rewarded positions (p = 0.69, ns). **(H)** %correct trials, when the subject transitions from a non-rewarded position to a rewarded position (p = 0.23, ns). **(I)** %errors, when the subject transitions from a non-rewarded position to another non-rewarded position (p = 0.13, ns).

exploring a previously rewarded target (T2) are illustrated in Fig. 5(**D**) and 5(**E**), respectively. Within the ensemble, IL single units detected in target intervals were analyzed in perievent raster plots. Given that the subject visits a target multiple times in each behavioral test trial (T1 or T2), the event (#) number for a single putative IL unit depicts spiking events (3 s before and 2 s after) for all intervals when the nose point is within a target pot for a behavioral task trial. By computing the perievent raster distribution, a perievent FR curve was derived for each putative IL unit. This represents the average of spiking events across all target intervals (event #) of a behavioral test trial, with standard deviation (Fig. 5(F-G)). Based on perievent spiking analysis that is centered (0 s) on reward acquisition at a target (T1) or exploration of a previously rewarded target (T2), the spontaneous FR (before), peak firing FR (during), and maintained FR (after) were derived.

Each mouse performed multiple experimental sessions, with randomized target locations, spaced several days apart (Fig. 5(A)). Thus, the results of putative IL principal neuron activity are presented as the

mean of FR for all IL units during trials (T1 or T2) in all sessions (raw). In addition, the mean of FR of IL units per mouse in each experimental trial of a session was also determined. It is noteworthy that both the raw mean FR and mean FR per mouse/trial show a similar pattern of change in directionality ( $\Delta$ FR) in statistical To analyses. standardize experimental conditions putative IL FR analysis. the spontaneous FR (i.e., FR at intervals not associated with a target non-target) or was compared for baseline reward acquisition and omission trials results (paired T-test). The showed that the spontaneous FR (Fig. 5(H), p = 0.59) and mean spontaneous FR per mouse/trial (p = 0.103) for IL putative cells were comparable for both trials across experimental sessions.

Multi-unit rasters for putative principal cell ensemble detected in the IL revealed a significant decrease in spiking at the time of reward acquisition (T1, Fig. 5(D)). Evidently, perievent raster and FR analysis of single IL units revealed a decrease in spiking for reward acquisition intervals at a target (event #) during behavioral task trials (Fig. 5(F)). Consequently, there was a decrease in the mean FR (Fig. 5(I), p < 0.0001) and FR mean per mouse/trial (p = 0.002) of IL putative units

during reward acquisition intervals in comparison with spontaneous FR and spontaneous FR/mouse trial. In subsequent omission trials (T2) when mice explored previously rewarded targets, IL putative units recorded a decrease in the mean FR (Fig. 5(J), p < 0.0001) and mean FR per mouse/trial (p < 0.0001) in comparison with the spontaneous FR scores.

These results show that IL representation of rewarded (T1) and reward-associated (T2) targets involve FR suppression. However, the threshold of IL FR suppression persisted for longer periods in reward acquisition intervals (Fig. 5(F,G)), compared with the exploration intervals of previously rewarded targets (T2). For intervals ( $\sim$ 2s) that immediately followed a reward acquisition event (T1), putative IL neurons exhibit a decrease in mean maintained FR (Figure, p < 0.0001) and maintained FR per mouse/trial (p = 0.012). Similarly, after exploring a reward-associated target (T2), putative IL units recorded a decrease in maintained FR (Fig. 5(L), p < 0.0001) and maintained FR per mouse/trial (p = 0.01). Together, these results show that putative IL

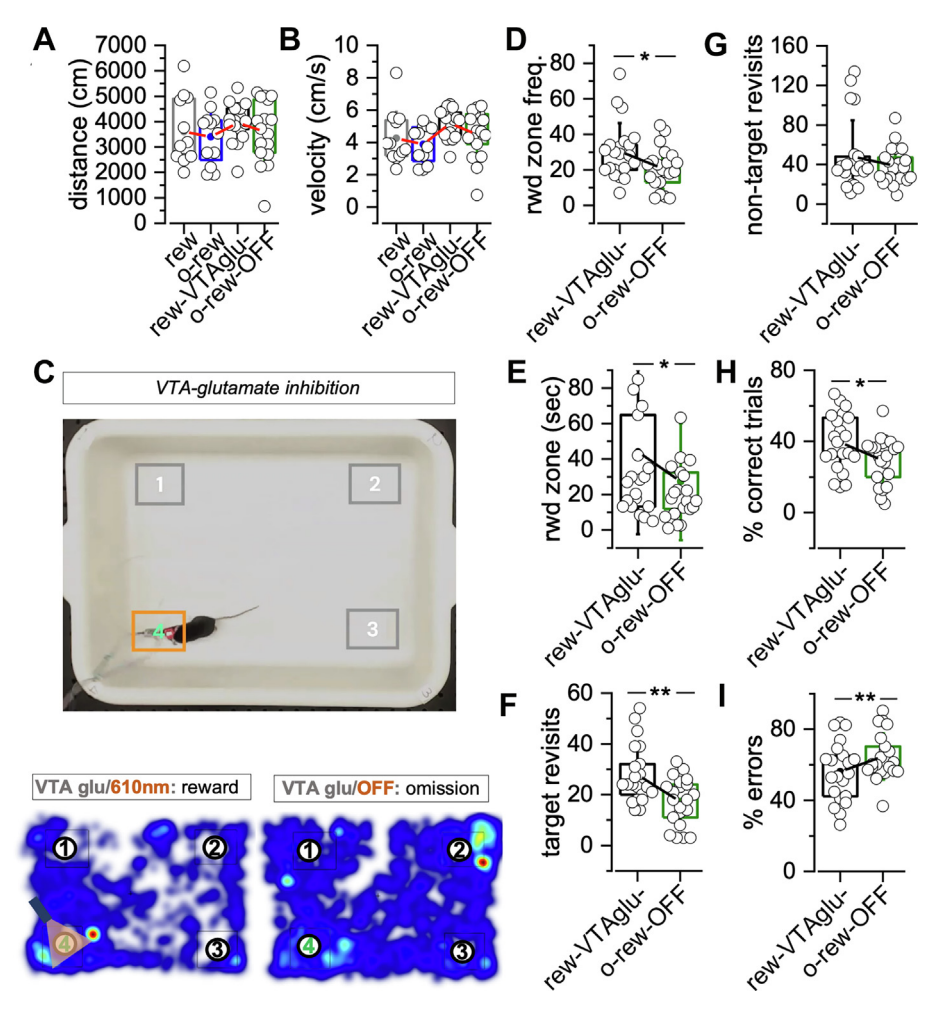


Fig. 3. VTA glutamate inhibition during reward acquisition increased habituation. One-Way ANOVA test shows no significant difference in the exploration ability of mice in reward or omission trials for baseline and VTA modulation sessions; (A) Mean distance covered (p > 0.05, ns). For this ANOVA test, F-value = 0.6344, DF = 3, and is not significant (p = 0.596). (B) Mean velocity (p > 0.05, ns). For this ANOVA test, DF = 3, F-value = 2.547, and is not significant (p = 0.065) (C) Sample heatmaps showing exploratory activity by a mouse during a reward acquisition task paired with VTA glutamate inhibition. In the omission trial, the subject did not show a preference for the previously rewarded target position 4. (D-E) The frequency (p = 0.03) and duration (p = 0.02) of reward zone visits decreased in omission trials that follow reward-acquisition trials paired with VTA glutamate inhibition (paired T-test). (F) Paired t-test comparison shows a significant decrease (p = 0.002) in the frequency of target re-visits in omission trials associated with previous VTA glutamate inhibition at the target position. (G) The frequency of re-visits to non-rewarded positions did not change significantly between reward acquisition and omission trials that involve VTA glutamate inhibition (p = 0.13, ns). (H) %correct trials, when the subject transitions from a non-rewarded position to a rewarded target, decreased with VTA glutamate inhibition (p = 0.0498). (I) %errors, when the subject transitions from a non-rewarded position to another non-rewarded position, increased with VTA glutamate inhibition (p = 0.008).

ensembles use FR suppression to encode behavioral events at rewarded targets, and subsequent events at the target when the reward is removed.

### $\Delta \text{FR}$ directionality is similar for reward and omission intervals

Putative IL principal cell ensembles encode the exploration of reward-linked targets primarily by FR suppression. Although most putative IL units exhibit a decrease in mean FR, subsets of neurons in the ensemble also exhibit an increase or have no change in

FR. Thus. to further ascertain if target events in reward acquisition (T1) and omission (T2) trials are encoded similarly, we compared the distribution of putative principal neurons based on directionality of the  $\Delta$ FR. This was determined as the percentage of fold change  $\Delta FR = (target interval)$ FR/spontaneous FR) x 100]. Thus, compared to the spontaneous FR, putative principal neurons with a 25% increase or decrease FR target intervals selected as having a change in FR. Neurons without a 25% change (increase or decrease) in FR were classified as having "no change in FR".

For the three baseline sessions (without **VTA** glutamate modulation) performed by n = 4mice, n = 44 putative principal were detected in the rewarded trials (T1) and n = 45cells in omission trials (T2). An average of 5 putative pyramidal units was detected per mouse in each trial. A significant percentage of the putative IL neurons show a decrease in FR during intervals of target exploration when a reward is presented (Fig. 6(A), T1: 81.8%, n = 36 cells) and subsequently omitted (Fig. 6(B), T2: 91.1%, n = 41 cells). Comparing the distribution of putative IL units based on  $\Delta FR$  directionality for reward acquisition and omission trials showed that  $\sim 10\%$  more neurons have FR decrease in exploration events target omission trials. Furthermore, target intervals of omission trials, there was a reduction in the percentage of neurons with increased FR (Fig. 6(B), T2: 2.2%, n = 1) when compared with the reward acquisition intervals (Fig. 6 (A), T1: 15.9%, n = 7). The

percentage of putative IL units without a change in FR increased in the target intervals of omission trials (T2: 6.7%, n=3) compared with rewarded intervals (T1: 2.3%, n=1).

Analysis of FR directionality based on the net  $\Delta$ FR in IL ensembles sampled for each mouse per trial and session supports the outcome for FR suppression during reward-linked target intervals. In reward acquisition trials (T1), 75% (n=9) of all mouse trials resulted in a decrease in the mean FR of putative IL neurons while 25% (n=3) of trials have a net increase

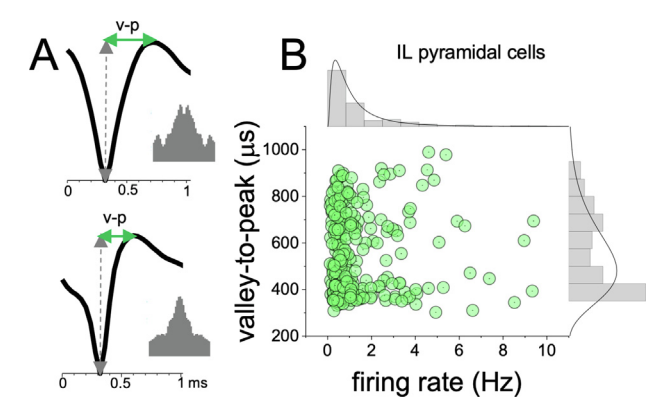


Fig. 4. Characterization of putative IL principal cells. (A) Sample waveform and autocorrelogram for putative IL units with wide and narrow v-p durations. (B) An edge histogram showing the distribution of putative IL principal cells based on waveform valley-to-peak time (v-p,  $\mu$ s) and the mean spontaneous FR (Hz).

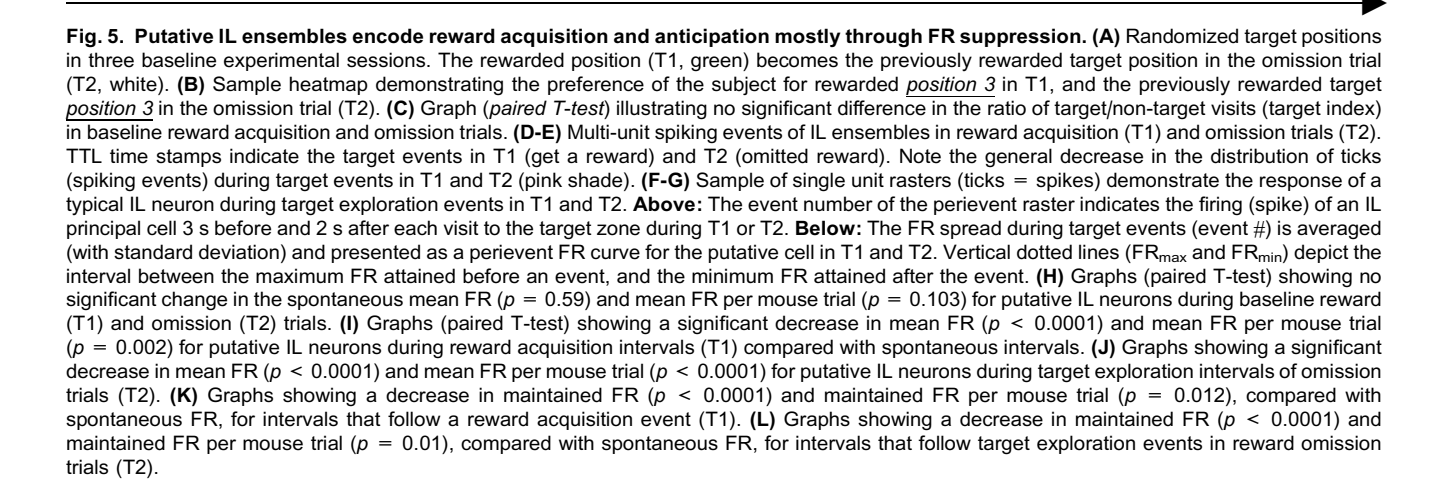
in FR (Fig. 6(C)). Interstingly, during subsequent exploration of the target without a target (T2), all (100%. n = 12) mouse trials resulted in a net decrease in putative IL FR (Fig. 6(D)). Because IL FR suppression encodes target events, when a reward (T1) is present and then subsequently omitted (T2), the mean of  $\Delta$ FR (Fig. 6(**E**), p = 0.098) and  $\Delta$ FR mouse/trial (Fig. 6(**F**), p = 0.14) are comparable for baseline sessions (T1 vs T2). Since the duration of FR suppression determines the fidelity of putative IL encoding of reward-oriented events, comparison of the Amaintained FR further demonstrates the similarity between ensemble representation of target intervals with a reward (T1), or associated with a reward (T2) (Fig. 6(G), p = 0.15). A similar outcome was observed when the maintained FR of putative IL neurons was analyzed per mouse trial (Fig. 6(H), p = 0.097).

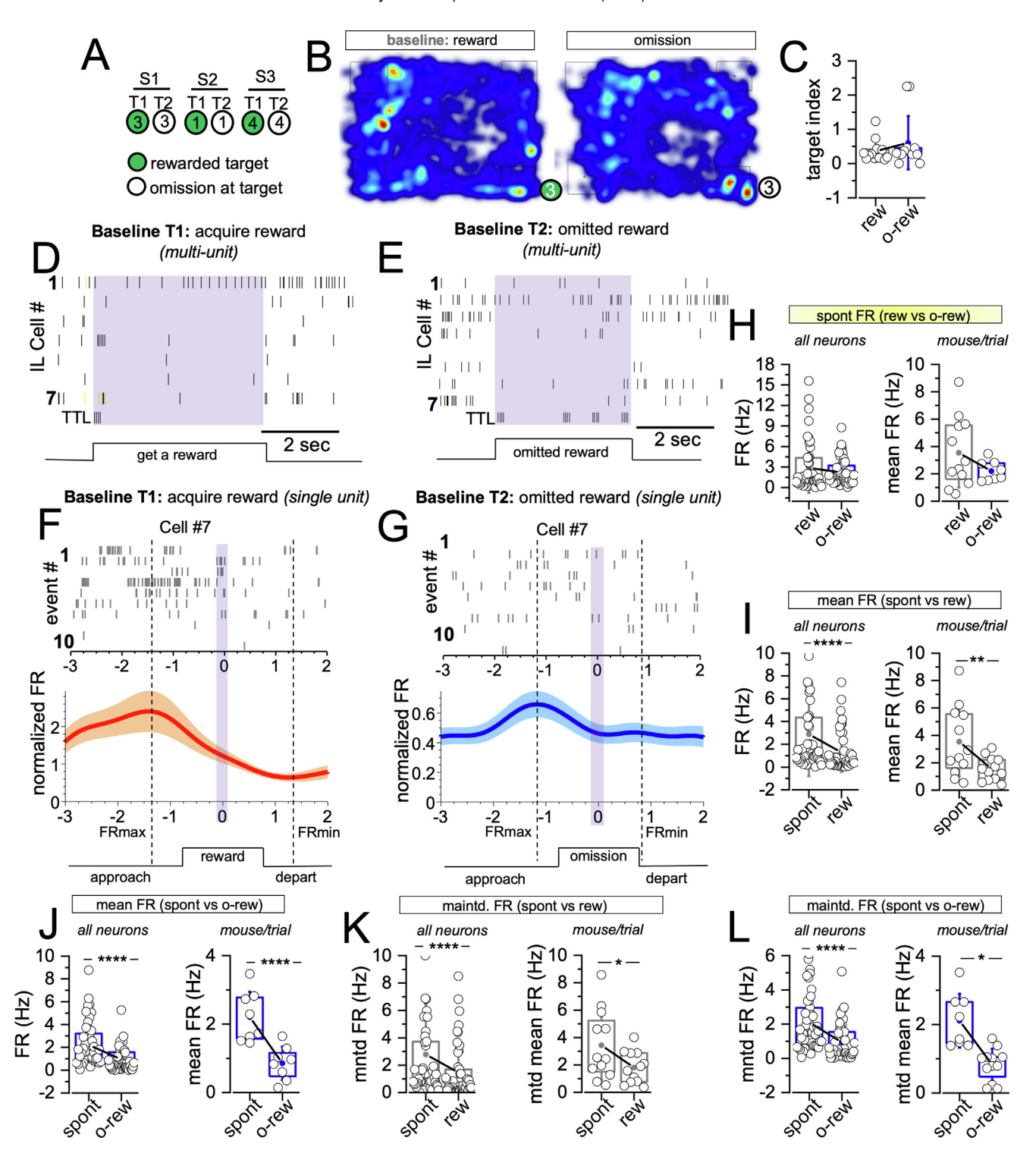
VTA glutamate inhibition alters IL firing pattern and reward-oriented behavioral expression. Inhibition of VTA glutamate neurons during reward acquisition intervals (Fig. 7(A)) decreased the frequency of target re-visits when the reward is present (T1: Movie 3), and subsequently omitted (T2: Movie 4). This lowered the

target index that represents the ratio of target to nontarget visits. In baseline sessions, the target index was comparable to reward acquisition, and subsequent omission trials (Fig. 5(C)). Interestingly, pairing reward acquisition with VTA glutamate inhibition led to a significant decrease in the target index for omission trials, compared with reward acquisition trials (Fig. 7(C), p = 0.012). As such, prior VTA glutamate inhibition during reward acquisition diminished the frequency of target re-visit when the reward is omitted. To standardize experimental conditions for comparing IL FR outcomes in baseline and VTA glutamate inhibition trials, we compared the spontaneous FR for all reward acquisition and omission trials (One-Way ANOVA). significant There was no difference in mean spontaneous FR (Fig.  $7(\mathbf{D})$ , p > 0.05. ANOVA  $F_{value} = 1.0561$ , DF = 3, and p = 0.368) and spontaneous FR per mouse (Fig. 7(E), p > 0.05. ANOVA  $F_{value} = 1.028$ , DF = 3, and p = 0.387) for all trials of baseline and VTA modulation sessions. Given that the same group of mice was used for all experimental sessions, a comparison of IL ensembles during baseline and VTA modulation sessions demonstrates the response of a fixed neuron population across experimental paradigms.

When reward acquisition is paired with VTA glutamate inhibition, IL ensembles exhibit a decrease in multi-unit spiking for the target intervals (Fig. 7(F)). Single-unit IL spikes sampled during reward acquisition intervals also show a decrease in FR around the target event (Fig. 7 (G)). Like baseline outcomes (Fig. 5(I)), putative IL units show a decrease in mean FR (Fig. 7(H), p < 0.0001) and mean FR per mouse/trial (p = 0.03) during reward acquisition intervals paired with VTA glutamate inhibition. Similarly, perievent rasters for putative IL multi-unit (Fig. 7(I)) and single-units (Fig. 7(J)), during target intervals of omission trials (T2- omission/610 nm OFF), revealed a decrease in mean FR (Fig. 7(K), p < 0.0001) and mean FR per mouse/trial (p = 0.00863).

Analysis of putative IL firing rate during target intervals revealed that VTA glutamate inhibition altered ensemble encoding of reward-linked events in two main ways.





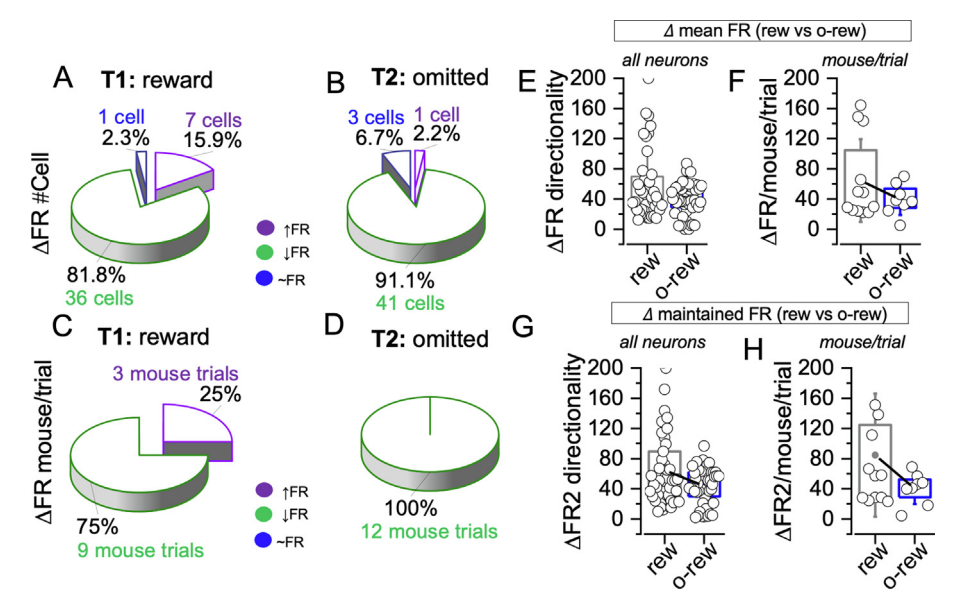
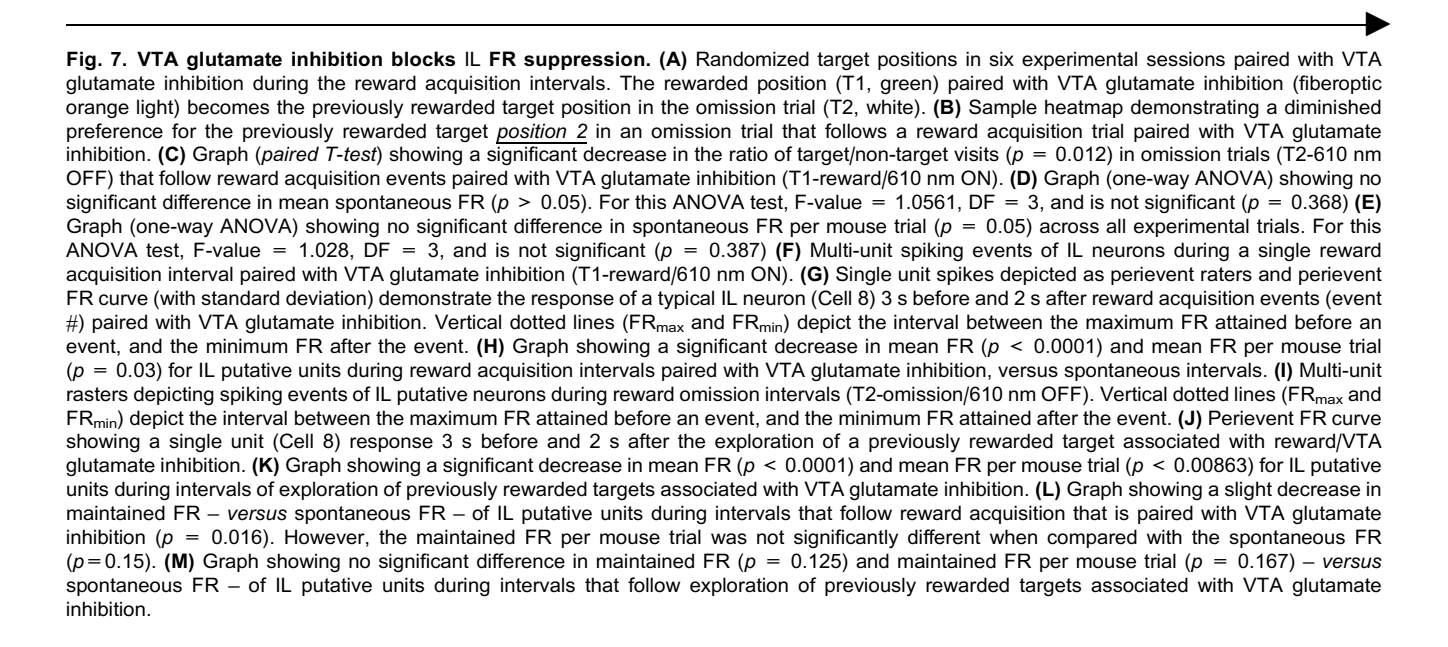


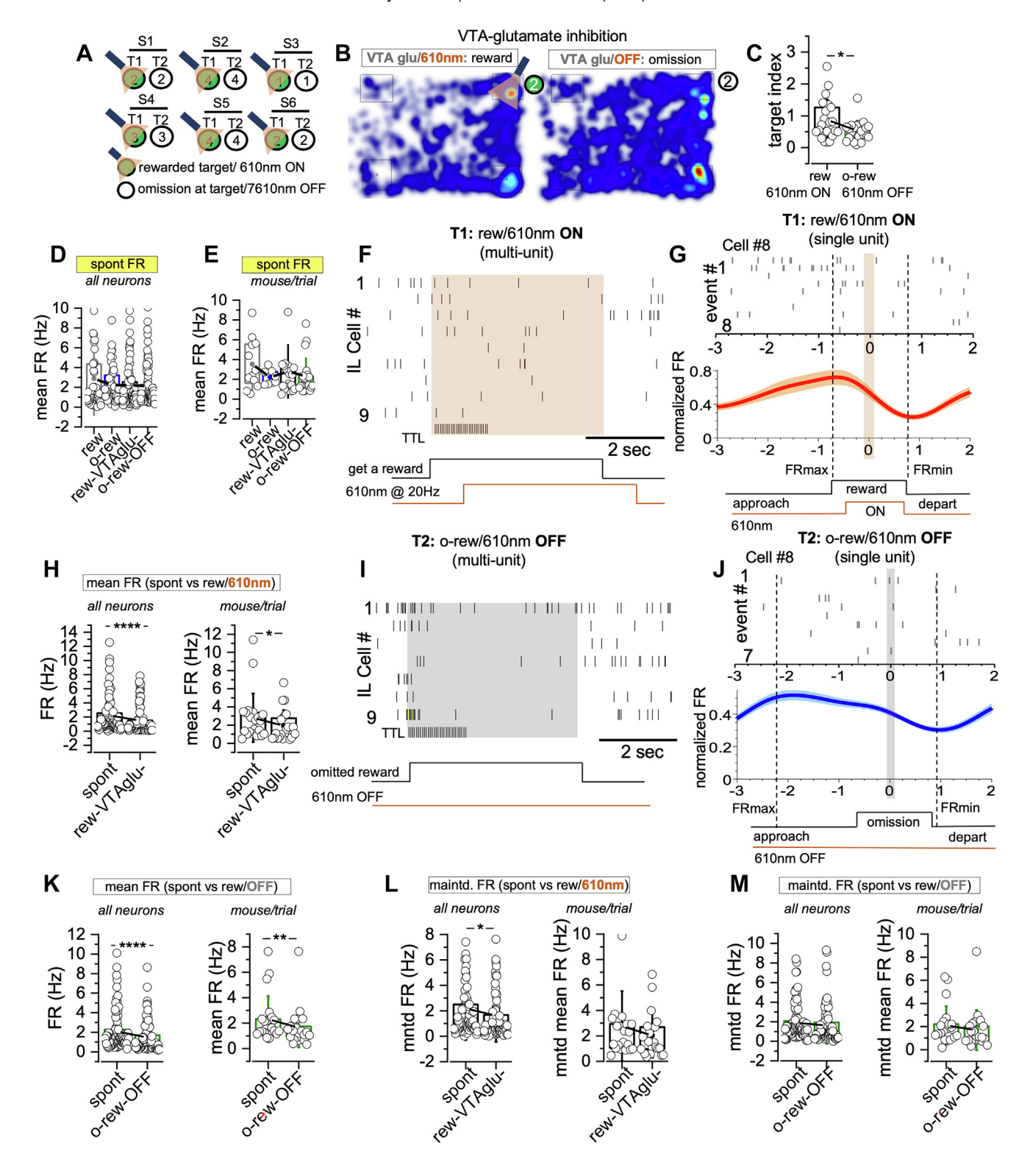
Fig. 6. IL ensembles encode reward-oriented target events through changes in the FR directionality of neuron subgroups. (A-B) Pie charts showing the percentage distribution of IL neurons determined by the directionality of  $\Delta$ FR (increase, decrease, or no change). The majority of IL neurons have FR suppression during reward acquisition (T1: 81.8%, n=36 cells) and reward omission intervals (91.1%, n=41 cells). (C-D) Pie charts showing the classification of mouse trials based on the mean  $\Delta$ FR directionality of IL neurons at target intervals. 75% of mouse trials show a decrease in FR (n=9) for IL neurons during reward acquisition intervals while 25% (n=3) have a mean increase in FR for the IL neurons. For all omission trials (T2, n=12), the mean FR for IL neurons shows a net decrease during the exploration of previously rewarded targets. (E-F) Graph showing no significant difference in  $\Delta$ FR directionality (p=0.098) and  $\Delta$ FR per mouse trial (p=0.14) for IL neurons when the rewarded and omission intervals are compared. (G-H) Graph showing no significant difference in  $\Delta$ maintained FR directionality ( $\Delta$ FR2).  $\Delta$ FR2 directionality (p=0.15) and  $\Delta$ FR2 per mouse trial (p=0.097) for IL neurons were comparable for intervals that follow the reward and omission intervals.

Firstly, the threshold of IL firing rate suppression, indicated by the fold change in  $\Delta$ FR, decreased during reward acquisition events paired with VTA glutamate inhibition (Fig. 7(**F-G**)), in comparison to similar intervals without VTA modulation (baseline, Fig. 5(**D-E**)).

Secondly. VTA glutamate inhibition during reward acquisition decreased the duration of FR suppression, moderately, after intervals target of T1reward/610 nm:ON, and robustly after target events in omission trials (T2-omission/610 nm:OFF). Specifically. after reward acquisition intervals of T1\_ reward/610 nm:ON, the maintained FR of putative IL units decreased (Fig. 7(L), p = 0.016) in comparison with spontaneous FRs. However, when the FR was compared per mouse/trial with corresponding spontaneous FR scores, there was no significant change (Fig. 7(L), p = 0.15). The most notable effect of pairing a reward with VTA glutamate inhibition was observed during omission trials where the weight of target-reward association reduced. Analysis of putative IL ensembles associated with these events revealed a sustained FR elevation around the target event (Fig.  $7(\mathbf{J})$ ). Consequently, the maintained FR (Fig. 7(**M**) p = 0.123) and maintained FR per mouse trial (p = 0.164) were significantly different comparison with spontaneous FR

scores. Together, these results indicate that VTA glutamate neurons are likely involved in the timing and duration of IL inhibition states that encode reward-linked events.

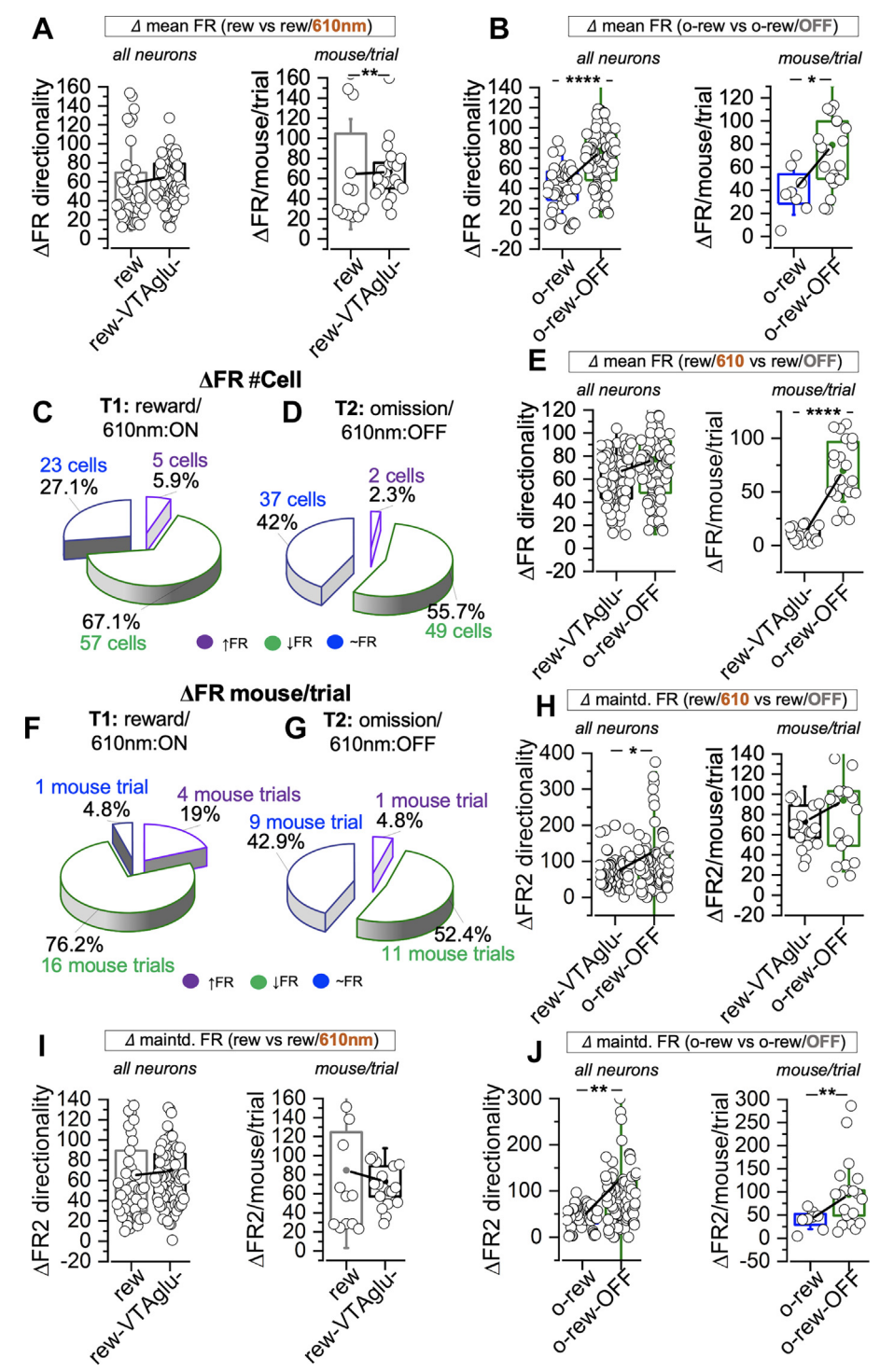




# VTA glutamate inhibition suppressed cortical inhibition threshold

Comparison of the  $\Delta$ FR directionality for the reward acquisition trials paired with VTA alutamate inhibition (T1reward/610 nm:ON) and subsequent omission trials (T2omission/610 nm:OFF) revealed significant changes the threshold firina rate suppression. Compared with baseline trials, VTA glutamate inhibition during reward acquisition did not significantly change the mean  $\Delta FR$  of all neurons sampled in putative IL ensembles (Fig. 8 (A), p = 0.455), supporting an overall decrease in FR for both intervals. However, analysis of ΔFR directionality per mouse/trial VTA glutamate showed that inhibition increased the count of mouse trials having a net increase in FR, compared with the baseline (p = 0.006). During target intervals of omission trials (T2omission/610 nm:OFF) associated with VTA glutamate inhibition, ΔFR directionality of IL putative ensembles was biased towards firing rate increase (Fig. 8(B), p < 0.0001). Likewise,  $\Delta FR$  of IL putative units sampled mouse/trial showed net  $\Delta$ FR that suggests an increased (p = 0.0116).

For the six baseline sessions performed by n = 4 mice, n = 85IL units were sampled in the rewarded trials paired with VTA alutamate inhibition (T1reward/610 nm:ON) and n = 88cells in the corresponding omission trials (T2omission/610 nm:OFF). During baseline reward acquisition intervals, a significant percentage of putative IL units show robust inhibition (Fig. **6(A)**, 81.8%). However, pairing reward acquisition with VTA glutamate inhibition reduced the percentage (14.7% decrease) of putative IL characterized by decrease (Fig. 8(C), T1: 67.1%, n = 57 cells). Furthermore, fewer putative (10% decrease) neurons have increased FR (T1: 5.9%, *n* cells) when 5



compared with baseline reward acquisition intervals without VTA glutamate inhibition (Fig. 6( $\bf A$ ), 15.9%). Interestingly, the distribution of putative IL neurons with no change in FR increased by 24.8% during reward events paired with VTA glutamate inhibition (T1: 27.1%, n=23 cells), in comparison with baseline reward events (Fig. 6( $\bf A$ ), T1: 2.3%, n=1 cell). Together, the results show that inhibition of VTA glutamate neurons reduces the frequency of target revisits and suppresses inhibition of putative IL ensembles. Notably, with VTA glutamate inhibition, there was a significant decrease in the percentage of IL neurons with firing rate suppression, while the distribution neurons with no change in FR increased.

In omission intervals associated with prior VTA glutamate inhibition and reward, 55.7% of putative neurons in IL ensembles were characterized by a firing rate decrease (Fig. 8(D), T2-omission/610 nm:OFF, n = 49 cells). This represents an 11.4% decrease in putative IL units with FR decrease when compared with the corresponding reward acquisition events that are paired with VTA glutamate inhibition (Fig. 8(C), T1reward/610 nm:ON, 67.1%, n = 57 cells). Compared to baseline omission trials (Fig. 6(B), T2: 91.1%), pairing VTA glutamate inhibition with reward acquisition caused a 35.4% reduction in IL putative units characterized by FR decrease during subsequent omission trials (Fig. 8 (**D**), T2-omission/610 nm:OFF, 55.7%, n = 49). In addition to a decrease in the distribution of putative IL neurons with FR suppression, the percentage of neurons without FR change during T2-omission/610 nm: OFF trials (42%, n = 37) increased by 14.9% in comparison with the reward acquisition trials paired with VTA glutamate inhibition (T1-reward/610 nm:ON, 27.1%, 23). Ultimately, comparing omission trials associated with prior VTA glutamate inhibition (T2omission/610 nm:OFF, 42%, n = 37) with baseline

omission trials (Fig. 6(**B**), T2: 6.7%, n=3), revealed a 35.3% increase in putative IL units without a change in FR.

Inhibiting VTA glutamate neurons during reward acquisition events at targets (T1-reward/610 nm:ON) reduced reward-target association. As a result, mice show a decrease in target index when the reward is omitted at target sites paired with VTA glutamate inhibition (Fig. 7(C), p = 0.012). In comparison with baseline tasks, mice show a sustained level of interest in the target when a reward is presented, then subsequently omitted (Fig. 5(C), p = 0.13). In baseline tasks, firing rate analysis for putative IL neurons revealed similar firing rate directionality for intervals where a reward is present (T1), and those that followed with the omission of rewards (T2) (Fig. 6(E), p = 0.098). Further analysis of these neurons per mouse trial further supports this outcome (Fig. 6(F), p = 0.14). Interestingly, putative IL ensembles show variations in FR directionality in behavioral events characterized by a reward-target index. Similar to the baseline, putative IL FR decreased for reward target intervals paired with VTA glutamate inhibition and their accompanying omission trials. Thus, the threshold of FR suppression was comparable for both intervals (Fig. 8 (**E**), all neurons, p = 0.705). However, there was an increase in the count of mouse trials with firing rate directionality that suggests a net increase in FR (Fig. 8 (E), mouse/trial, p < 0.0001) for omission trials linked to prior VTA glutamate inhibition. From these results, it is inferred that pairing a reward with VTA glutamate inhibition reduced reward-target association, and is represented as sustained loss of FR suppression in putative IL ensembles.

Further analysis of  $\Delta$ FR directionality per mouse/trial showed that VTA glutamate inhibition significantly reduced putative IL inhibition states during reward

Fig. 8. VTA glutamate inhibition alters ΔFR directionality of IL neurons around reward-oriented target events: (A) Graphs showing no significant difference in the directionality of  $\Delta$ FR for putative IL neurons (p = 0.455) sampled in baseline reward events, and reward intervals paired with VTA glutamate inhibition. The ΔFR for putative IL neuron per mouse trials (p = 0.006) indicated FR increase during reward events paired VTA glutamate inhibition. (B) Graphs showing  $\Delta$ FR directionality that indicates a predominant FR increase for IL neurons (p < 0.0001) and mouse trials (p = 0.0116) during the exploration of previously rewarded targets associated with VTA glutamate inhibition. (C-D) Pie charts showing the percentage distribution of putative principal cells determined by the directionality of  $\Delta$ FR (increase, decrease, or no change) in IL ensembles. A significant percentage of IL neurons exhibits FR suppression during reward acquisition interval paired with VTA glutamate inhibition (T1-reward/ 610 nm ON: 67.1%, n = 57 cells) and subsequent intervals for exploration of previously rewarded targets (T2-omission/610 nm OFF: 55.7%, n = 49 cells). The percentage distribution of putative cells with FR decrease is lower for VTA glutamate inhibition trials when compared with the baseline reward (Fig. 6(A), T1: 81.8%, n=36 cells) and omission (Fig. 6(B), 91.1%, n=41 cells) trials. (E) Graph showing no significant change in ΔFR directionality (p = 0.705) putative IL cells during reward acquisition intervals paired with VTA glutamate inhibition, versus subsequent omission intervals. The  $\Delta$ FR for putative IL neurons per mouse trials (p < 0.0001) depicts FR increase that is significant in omission intervals associated with reward/VTA glutamate inhibition trials. (F) Pie charts showing the classification of mouse trials based on the mean ΔFR directionality of IL neurons at target intervals. 76.2% of mouse trials show a decrease in FR (n = 16) for IL neurons during reward acquisition intervals paired with VTA glutamate inhibition. Four mouse trials (19%) show an increase and one mouse trial with no change in FR (4.8%). (G) Pie chart showing a significant reduction in the percentage of mouse trials with a net FR decrease for IL neurons (52.4%, 11 mouse trials). The percentage of mouse trials with no change in FR of IL neurons increased (42.1%, nine mouse trials). One mouse trial had a net FR increase (4.8%). (H) Graphs showing an increase in maintained FR ( $\Delta$ FR2) directionality (p = 0.032) for IL putative neurons during T2-omission/610 nm OFF target (omission) intervals compared with the associated reward acquisition intervals (T1-reward/610 nm ON). The  $\Delta$ FR2 per mouse trial was comparable (p = 0.218) for both T1-reward/ 610 nm ON and T2-omission/610 nm OFF. T2-omission/610 nm OFF was empirically higher. (I) Graph showing no significant change in ∆FR2 directionality for IL neurons during intervals that follow reward acquisition events, with and without VTA glutamate inhibition (p = 0.369),  $\Delta$ FR2 directionality per mouse trial is also not significantly different (p = 0.64). (J) Graphs showing a significant increase in maintained FR directionality for IL neurons (p = 0.003) and mouse trials (p = 0.005) for omission trials paired with prior VTA glutamate inhibition, versus the baseline.

acquisition intervals. As such the mean of firing rate directionality demonstrates an increase in FR for reward intervals paired with VTA glutamate inhibition, compared with the baseline (Fig. 8(A), mouse/trial, p = 0.006). The distribution of mouse trials with firing rate suppression was also comparable for baseline (Fig. 6 (C), T1: 75%) and VTA modulation (Fig. 8(F), T1reward/610 nm ON: 76.2%). Furthermore, in 25% (T1) and 19% (T1-reward/610 nm ON) of trials, putative IL neurons showed an increased mean FR. However, for target intervals of omission trials, pairing a reward with VTA glutamate inhibition caused a significant decrease in the percentage of mouse trials with firing suppression when compared with the baseline (Fig. mouse/trial, p = 0.0116). In baseline omission trials (Fig. 6(D), T2), putative IL ensembles show a net absolute FR suppression in all mouse trials (Fig. 6(D), 100%). Conversely, the percentage of mouse trials with net FR suppression decreased to 52.4% (Fig. 8(G), T2omission/610 nm OFF) for omission trials associated with prior VTA glutamate inhibition. Furthermore, there is a percentage increase in mouse trials with no net change in  $\Delta$ FR directionality (42.9%) and those with elevated FR (4.8%). These results support the effect of VTA glutamate inhibition on IL encoding of rewardtarget association.

Although IL ensembles encode reward-linked target events through net FR suppression, perievent raster analysis showed that the timing and duration of FR suppression were mostly altered in the omission trial that followed a reward acquisition event paired with VTA glutamate inhibition. As such in omission trials associated with prior VTA glutamate inhibition, putative neurons show a net elevation in Amaintained FR (Fig. 8 (H), p = 0.032) and not the maintained FR per mouse trial ( $\Delta$ FR2; p = 0.218, ns), when compared with corresponding reward acquaition intervals. It follows that the VTA glutamate inhibition did not significantly change the maintained FR associated with the target intervals of reward acquisition trials. Thus, Amaintained FR directionality (Fig. 8(I), p = 0.369) and  $\Delta$ FR2 of putative IL neurons per mouse trial (p = 0.64) were comparable for baseline and VTA glutamate-linked reward acquisition intervals. However, as shown above, the most notable changes in Δmaintained FR and ΔFR2 per mouse trial were observed for target events of omission trials that followed reward acquisition trials paired with VTA glutamate inhibition. Thus, Δmaintained FR (Fig. 8 (J), p = 0.003) and  $\Delta$ maintained FR per mouse trial (p = 0.005) were significantly higher for omission events that follow VTA glutamate inhibition, in comparison with the baseline.

#### **DISCUSSION**

The mPFC is a neocortical region that governs cognitive function and executive behavior (Euston et al., 2012; Ferenczi et al., 2016; Capuzzo and Floresco, 2020; Anastasiades and Carter, 2021; Coley et al., 2021; Green and Bouton, 2021; Hardung et al., 2021). A key aspect of

the mPFC function is the processing of various contexts to moderate executive behavioral responses to environmental stimuli (Moorman and Aston-Jones, 2015; Hardung et al., 2021). This process is broadly facilitated by reciprocal connections between the VTA and cognitive centers like the hippocampus and mPFC (Lisman and Grace, 2005; Moorman and Aston-Jones, 2015; Hu, 2016: Nett and LaLumiere, 2021). The VTA is a heterogeneous midbrain nucleus in the mesocorticolimbic pathway that contains dopamine, glutamate, and GABA neurons (Lisman and Grace, 2005; Ntamati and Luscher, 2016; Bouarab et al., 2019; Montardy et al., 2019; Han et al., 2020). While VTA neurons innervate several brain centers. the distribution of the terminals based on neurotransmitter type is usually biased between the dopamine and nondopamine components, depending on the target site (Yoo et al., 2016; Breton et al., 2019). In addition to dopamine and GABA inputs, VTA projections to the mPFC PrL and IL regions contain the VTA glutamate-mPFC tract (Yoo et al., 2016; Park and Moghaddam, 2017; Perez-Lopez et al., 2018; Breton et al., 2019; Montardy et al., 2019).

In cortical control of behavioral expression, previous studies suggest a robust functional dichotomy between sub-populations of mPFC neurons in the PrL and IL. There is a consensus that the PrL is involved in goal-oriented task learning while the IL neurons are central to behavioral suppression (Euston et al., 2012; Moorman and Aston-Jones, 2015; Moorman et al., 2015; Nakayama et al., 2018; Riaz et al., 2019; Nett and LaLumiere, 2021). While this hypothesis has been tested with great certainty in fear-driven behavior, there is less agreement about the applicability of this concept in reward-oriented tasks.

Recent studies aimed at understanding dissociation of the hypothesis in reward-linked behavior demonstrate two major findings. First, the change in the firing rate of putative mPFC neurons in response to rewarding and non-rewarding stimuli is not entirely dichotomous, rather, the subpopulation of neurons in the PrL and IL respond in a variety of ways (FR increase, decrease, or no change) that weighs the probability of "getting a reward". Interestingly, subsets of neurons were also activated by both rewarding and nonrewarding contexts (Moorman and Aston-Jones, 2015; Moorman et al., 2015). It follows that PrL neurons in reward-oriented tasks were biased toward an increased FR while IL responses were biased toward inhibition (Moorman and Aston-Jones, 2015). Furthermore, the response of VTA and mPFC neuronal ensembles is synchronized in reward-oriented tasks. Interestingly, the synchrony is flexible and can be adjusted when the reward is associated with other variables such as the risk of punishment (Park and Moghaddam, 2017). These concepts suggest that mPFC neurons encode reward-oriented tasks through population dynamics, and the distribution of neuron sub-sets with various response patterns depicts the possible state of interaction between the mPFC and VTA neurons (Park and Moghaddam, 2017).

The current study examined FR dynamics of putative IL ensembles during reward-oriented tasks that read out

the expression of food-seeking foraging behavior in mice. By combining in vivo neural recording with optogenetic modulation of VTA neurons, the role of brain-wide excitatory VTA inputs was assessed in the expression of reward-oriented behavior, and IL encoding of events that involve acquiring, then missing a reward at a specific target location. The results show that the majority of putative neurons IL ensembles use FR suppression in encoding reward acquisition and subsequent exploration of previously rewarded targets. However, pairing reward acquisition with VTA glutamate inhibition reduced the weight of reward-target association when the reward was omitted subsequently. This was represented as a significant loss of FR suppression in IL ensembles, and a decrease in the duration of such suppression.

# Suppression of mPFC FR encodes reward acquisition and anticipation

Previous studies showed that VTA glutamate neurons respond to both reward and aversive stimuli (Park and Moghaddam, 2017; Montardy et al., 2019), and are involved in valence determination (Yoo et al., 2016; Montardy et al., 2019; Han et al., 2020). Here, we showed that activation of VTA glutamate neurons during reward acquisition is pertinent for reward-target association which depicts the affinity for previously rewarded targets in omission trials (Fig. 3). To this extent, selective inhibition of VTA glutamate neurons during reward acquisition reduced the frequency of target exploration (Fig. 7(C) (compared to a similar task without VTA glutamate inhibition (baseline, Fig. 5(C)). These results indicate that reward acquisition and subsequent preference for previously rewarded targets are - in part - dependent on VTA glutamate activity.

Pairing reward acquisition and VTA glutamate inhibition caused an empirical decrease in reward acquisition (T1), and a significant decrease in reward-target association (T2). Since the expression of reward-seeking behavior is governed by IL activity suppression (Moorman and Aston-Jones, 2015; Riaz et al., 2019; Hardung et al., 2021; Nett and LaLumiere, 2021), these results suggest that activation of VTA glutamate neurons during reward acquisition intervals bolster positive valence association by enhancing putative IL FR suppression. As such, when re-exploring a target without a reward or VTA glutamate inhibition, mice showed less affinity which suggests a reduction in the weight of the "reward-target association".

In baseline tasks (without VTA glutamate inhibition), putative IL ensembles encode reward-oriented exploratory behavior through FR suppression during target interval, and persistence of the inhibition states after the target event (maintained FR). It follows that both the reward acquisition intervals (T1) and target intervals in omission trials (T2) are encoded by these mechanisms. Therefore, the  $\Delta$ mean FR (Fig. 6(E-F)) and  $\Delta$ maintained FR (Fig. 6(G-H)) were comparable for intervals of reward acquisition (T1), and exploration of previously rewarded targets (T2). In support of this proposition, the percentage distribution of putative IL

neurons and mouse trials characterized by FR decrease were comparable for reward acquisition and subsequent omission trials.

# A novel reward-driven task for assessing neural assemble dynamics

The goal of the behavioral task was to determine the population dynamics for IL principal neurons when a food reward is encountered, compared to when the reward is intentionally omitted after 45 min. We sought to determine if the IL cells – through their change in FR patterns – distinguish between a reward that is obtained (T1) and the chance that a reward may be obtained at a particular location. To answer the question about reward seeking, a training session was performed at 48 h, then 24 h before the first test. During the training session, animals obtained a reward at all four sites thus learning that the pots were meant for food rewards. For the experimental trials, animals were also fasted to motivate foraging behavior.

The sample size is n=4. However, these animals have implants. So, each animal performed the behavioral test three times during the baseline period (no VTA modulation), and six times in VTA modulation experiments. By considering ensembles in each mouse and trial, robust averages were derived for each neuron, then mouse trials. Importantly, using the same set of animals for all experiments provides a premise for comparing a relatively fixed neural ensemble across experimental conditions. Here, the baseline experiment is the "control" and VTA modulation sessions are the "treatment". For this reason, each mouse served as its control.

Using Ethovision XT15 with hardware control module synchronized behavioral events at the reward pots with the sampled IL continuous spike train. Since the floor and edges of the reward pots were marked as virtual zones, the behavioral tracking software detected events when the tracked nose point crossed the edge and reached the floor. This is ideal for animals with implants and tethers since the wires and optic fiber cables can limit the depth of head movement. Thus, having reward on edge and center is preferred for this experiment. By placing reward pots in four corners of the test chamber, there is a premise to derive simple yes or no outputs when analyzing electrophysiological data derived from IL ensembles. It follows that the location of each reward pot represents a spatial context because the pots are uniform, and only differ in their location. The wall is also uniform. Therefore, the task is reliant on spatial navigation of the space.

Reward-seeking, in this context, describes foraging behavior after the animal has been trained, and then fasted. Thus, there is motivation to find food - which is the reward for expressing foraging behavior. Reward-seeking, per this experiment, indicates getting a reward (T1) or exploring a previously rewarded site when the reward is omitted (T2). If the animal re-visited the reward sites many times and finished it, more was added during the task. To maintain the novelty of the task, a 3-day rest period was allowed in between sessions such that the target location is randomized across experimental sessions. When a mouse gets a

reward in T1, they are motivated to return more frequently to that location in T2 knowing there is a chance of consuming food reward. This behavioral phenotype was observed for all baseline sessions and suggests that animals associated the target pot with a reward. Ultimately, determining the change in FR of IL ensembles during T1-T2 created a link between neural parameters and behavioral outcomes when a reward is presented, then subsequently omitted at a target.

To control the experiments, in Fig. 5(H) the spontaneous FR of IL putative neurons was compared when animals performed T1 (reward) and T2 (omitted) of the baseline session. The spontaneous FR was determined for intervals wherein the animal was not near a target pot. The spontaneous FR was compared in two ways: (i) the spontaneous FR of all neurons. detected in all animals, for all sessions was compared for T1 and T2. There was no significant difference as shown in Fig. 5(H) (left pane). Similarly, the average spontaneous FR for putative pyramidal cells in IL ensembles was not significantly different considered per mouse trial for each session (right pane). These results indicate that for these tasks. the basal activity of IL neurons did not change across sessions. This is further evident as no change in spontaneous FR when all experiment types were compared (Fig. 7(D)-(E): baseline T1 & T2, and VTA modulation T1 & T2) for the baseline and modulation sessions. To examine how the  $\Delta FR$  occurs over a spread of time, the FR of neurons was measured around a target event using perivent curves. As such for a target event, the spontaneous FR before an approach, was compared with the peak FR (during the event), and the maintained FR (immediately after the event).

### VTA glutamate inhibition decreased reward-seeking behavior

Selective inhibition of VTA glutamate neurons did not significantly lower reward acquisition, however, an empirical decrease was observed. Interestingly, its impact was most notable as a decrease in the exploration of targets when the reward was omitted subsequently (Fig. 3). Our results show that FR suppression in putative IL ensembles was comparable for reward acquisition intervals with and without VTA glutamate inhibition. However, when considered per mouse trial, pairing rewarded target events with VTA glutamate inhibition resulted in a net increase in FR for most mouse trials (Fig. 8(A), p = 0.006). Similarly, the Δmaintained FR for intervals that follow the reward acquisition events were also comparable suggesting that the duration of FR suppression was not significantly altered (Fig. 8(I)). However, in omission trials that follow reward acquisition events paired with VTA glutamate inhibition, putative IL inhibition threshold, and duration of FR suppression were significantly impacted. Notably, there was a reduction in the percentage of IL neurons with FR decrease, and higher count of putative neurons with no change in FR during omission trials associated with prior VTA glutamate inhibition (Fig. 8(D,G)). As a result, the mean  $\Delta FR$  directionality and  $\Delta FR$ 

directionality per mouse trial revealed a shift towards FR increase in putative IL ensembles for these omission trials, compared with baseline trials (Fig. 8(B)). Furthermore, the threshold of FR suppression for these omission intervals decreased significantly when the associated reward-acquisition interval was paired with VTA glutamate inhibition (Fig. 8(J)). As such, with VTA glutamate inhibition, the  $\Delta$ maintained FR scores showed a sustained FR increase for the period that follows a target event, compared with baseline sessions.

These results agree with recent studies that demonstrate diverse firing patterns for neuron sub-sets in mPFC ensembles (Moorman and Aston-Jones, 2015: Moorman et al., 2015: Park and Moghaddam, 2017: Jacobs and Moghaddam, 2020: Nett and LaLumiere. 2021). In baseline sessions. ΔFR analysis showed that a significant percentage of the sampled putative IL neurons have a decrease in FR when animals acquire a reward and subsequently explore the same target without the reward. Thus, the net decrease in the firing rate of IL ensembles during reward-acquisition events is a cumulation of FR suppression for most IL neurons ( $\sim$ 82%), with other subsets having no change (2.3%) or an increase in FR (15.9%). Although VTA glutamate inhibition did not significantly change the directionality of the FR during reward acquisition, it empirically lowered the count of neurons characterized by FR suppression (67.1%) in the omission trials that followed. Furthermore, VTA glutamate inhibition was associated with an increased percentage of putative IL neurons without change in FR. Taken together, it is likely that VTA glutamate inhibition, during reward acquisition, lowered reward-target association by attenuating FR suppression in IL ensembles when a reward is omitted subsequently from the same target.

A limitation of this study is that the expression of inhibitory opsin in VTA Valut2<sup>Cre</sup> neurons does not distinguish between glutamate neurons and some populations of dopamine neurons that co-release glutamate (Perez-Lopez et al., 2018; Montardy et al., 2019; Han et al., 2020). However, it is expected that a significant percentage of the modulated VTA neurons are glutamate-releasing neurons. Previous studies have shown that VTA neurons project directly to the infralimbic and prelimbic cortex, and indirectly through brain regions like the nucleus accumbens that modulate the mPFC (Ferenczi et al., 2016; Nakayama et al., 2018; Coley et al., 2021; Hardung et al., 2021). Therefore, behavioral changes during inhibition of VTA glutamate neurons in the VTA involve both direct and indirect effects exerted on the IL. In future studies, combined recording in prelimbic and infralimbic regions during VTA glutamate modulation can determine if VTA glutamate inputs gate the firing of the two regions and produce a dichotomous behavioral response in feardriven experiments. Also, future studies could address the direct inhibition of VTA glutamate terminals in the mPFC.

#### **SUMMARY**

Suppression of principal cell FR is an encoding mechanism for reward-oriented exploratory behavior. As such, a significant population of putative IL neurons

exhibits FR decrease when a reward is presented at a target or omitted subsequently at the same target. The results showed that the exploration of targets and the accompanying cortical FR suppression in reward-oriented tasks are strongly linked to the broad activation of VTA glutamate neurons. As such, VTA glutamate inhibition decreased the frequency of target exploration and is accompanied by a decrease in the threshold of IL FR suppression. Together, we conclude that VTA glutamate neurons are likely involved in determining the weight of reward-target association for previous reward encounters.

#### **AUTHOR CONTRIBUTION**

OOM and AT designed the experiments. OOM, AT, and TBV performed the recording procedures. OOM analyzed the results. OOM and AT prepared the manuscript.

#### **ACKNOWLEDGMENT**

This work is funded by National Science Foundation Grant (IOS 2137023) awarded to OOM.

#### REFERENCES

- Anastasiades PG, Carter AG (2021) Circuit organization of the rodent medial prefrontal cortex. Trends Neurosci. 44:550–563.
- Bartho P, Hirase H, Monconduit L, Zugaro M, Harris KD, Buzsaki G (2004) Characterization of neocortical principal cells and interneurons by network interactions and extracellular features. J. Neurophysiol. 92:600–608.
- Bouarab C, Thompson B, Polter AM (2019) VTA GABA neurons at the interface of stress and reward. Front. Neural Circuits 13:78.
- Breton JM, Charbit AR, Snyder BJ, Fong PTK, Dias EV, Himmels P, Lock H, Margolis EB (2019) Relative contributions and mapping of ventral tegmental area dopamine and GABA neurons by projection target in the rat. J Comp Neurol 527:916–941.
- Brischoux F, Chakraborty S, Brierley DI, Ungless MA (2009) Phasic excitation of dopamine neurons in ventral VTA by noxious stimuli. PNAS 106:4894–4899.
- Broussard JI, Yang K, Levine AT, Tsetsenis T, Jenson D, Cao F, Garcia I, Arenkiel BR, Zhou FM, de Biasi M, Dani JA (2016) Dopamine regulates aversive contextual learning and associated in vivo synaptic plasticity in the hippocampus. Cell Rep. 14:1930–1939.
- Capuzzo G, Floresco SB (2020) Prelimbic and infralimbic prefrontal regulation of active and inhibitory avoidance and reward-seeking. J. Neurosci. 40:4773–4787.
- Chau DT, Roth RM, Green AI (2004) The neural circuitry of reward and its relevance to psychiatric disorders. Curr. Psychiatry Rep. 6:301–309
- Chen YH, Wu JL, Hu NY, Zhuang JP, Li WP, Zhang SR, Li XW, Yang JM, Gao TM (2021) Distinct projections from the infralimbic cortex exert opposing effects in modulating anxiety and fear. J. Clin. Invest. 131.
- Chung JE, Magland JF, Barnett AH, Tolosa VM, Tooker AC, Lee KY, Shah KG, Felix SH, Frank LM, Greengard LF (2017) A fully automated approach to spike sorting. Neuron 95:1381–1394 e6.
- Coley AA, Padilla-Coreano N, Patel R, Tye KM (2021) Valence processing in the PFC: reconciling circuit-level and systems-level views. Int. Rev. Neurobiol. 158:171–212.

- Duszkiewicz AJ, McNamara CG, Takeuchi T, Genzel L (2019) Novelty and dopaminergic modulation of memory persistence: a tale of two systems. Trends Neurosci. 42:102–114.
- Euston DR, Gruber AJ, McNaughton BL (2012) The role of medial prefrontal cortex in memory and decision making. Neuron 76:1057–1070.
- Ferenczi EA, Zalocusky KA, Liston C, Grosenick L, Warden MR, Amatya D, Katovich K, Mehta H, Patenaude B, Ramakrishnan C, Kalanithi P, Etkin A, Knutson B, Glover GH, Deisseroth K (2016) Prefrontal cortical regulation of brainwide circuit dynamics and reward-related behavior. Science 351 aac9698.
- Floresco SB, Todd CL, Grace AA (2001) Glutamatergic afferents from the hippocampus to the nucleus accumbens regulate activity of ventral tegmental area dopamine neurons. J. Neurosci. 21:4915–4922.
- Ford CP, Williams JT (2008) Mesoprefrontal dopamine neurons distinguish themselves. Neuron 57:631–632.
- Funahashi S (2017) Working memory in the prefrontal cortex. Brain Sci. 7.
- Ghanbarian E, Motamedi F (2013) Ventral tegmental area inactivation suppresses the expression of CA1 long term potentiation in anesthetized rat. PLoS One 8:e58844.
- Green JT, Bouton ME (2021) New functions of the rodent prelimbic and infralimbic cortex in instrumental behavior. Neurobiol. Learn. Mem. 185 107533.
- Han Y, Zhang Y, Kim H, Grayson VS, Jovasevic V, Ren W, Centeno MV, Guedea AL, Meyer MAA, Wu Y, Gutruf P, Surmeier DJ, Gao C, Martina M, Apkarian AV, Rogers JA, Radulovic J (2020) Excitatory VTA to DH projections provide a valence signal to memory circuits. Nat. Commun. 11:1466.
- Hardung S, Jackel Z, Diester I (2021) Prefrontal contributions to action control in rodents. Int. Rev. Neurobiol. 158:373–393.
- Hoover WB, Vertes RP (2007) Anatomical analysis of afferent projections to the medial prefrontal cortex in the rat. Brain Struct. Funct. 212:149–179.
- Hu H (2016) Reward and aversion. Annu. Rev. Neurosci. 39:297–324.
- Ishikawa A, Ambroggi F, Nicola SM, Fields HL (2008) Contributions of the amygdala and medial prefrontal cortex to incentive cue responding. Neuroscience 155:573–584.
- Jacobs DS, Moghaddam B (2020) Prefrontal cortex representation of learning of punishment probability during reward-motivated actions. J. Neurosci. 40:5063–5077.
- Jonkman S, Mar AC, Dickinson A, Robbins TW, Everitt BJ (2009) The rat prelimbic cortex mediates inhibitory response control but not the consolidation of instrumental learning. Behav. Neurosci. 123:875–885.
- Lammel S, Lim BK, Malenka RC (2014) Reward and aversion in a heterogeneous midbrain dopamine system. Neuropharmacology 76(Pt B):351–359.
- Lisman JE, Grace AA (2005) The hippocampal-VTA loop: controlling the entry of information into long-term memory. Neuron 46:703–713.
- Liu C, Kaeser PS (2019) Mechanisms and regulation of dopamine release. Curr. Opin. Neurobiol. 57:46–53.
- Luscher C, Malenka RC (2011) Drug-evoked synaptic plasticity in addiction: from molecular changes to circuit remodeling. Neuron 69:650–663.
- McNamara CG, Tejero-Cantero A, Trouche S, Campo-Urriza N, Dupret D (2014) Dopaminergic neurons promote hippocampal reactivation and spatial memory persistence. Nat. Neurosci. 17:1658–1660.
- Montardy Q, Zhou Z, Lei Z, Liu X, Zeng P, Chen C, Liu Y, Sanz-Leon P, Huang K, Wang L (2019) Characterization of glutamatergic VTA neural population responses to aversive and rewarding conditioning in freely-moving mice. Sci. Bull. 64:1167–1178.
- Moorman DE, Aston-Jones G (2015) Prefrontal neurons encode context-based response execution and inhibition in reward seeking and extinction. PNAS 112:9472–9477.

- Moorman DE, James MH, McGlinchey EM, Aston-Jones G (2015) Differential roles of medial prefrontal subregions in the regulation of drug seeking. Brain Res. 1628:130–146.
- Nakayama H, Ibanez-Tallon I, Heintz N (2018) Cell-type-specific contributions of medial prefrontal neurons to flexible behaviors. J. Neurosci. 38:4490–4504.
- Nett KE, Lalumiere RT (2021) Infralimbic cortex functioning across motivated behaviors: can the differences be reconciled? Neurosci. Biobehav. Rev. 131:704–721.
- Ntamati NR, Luscher C (2016) VTA projection neurons releasing GABA and glutamate in the dentate gyrus. eNeuro:3.
- Oler JA, Fudge JL (2019) A tale of two pathways. Elife 8.
- Park AJ, Harris AZ, Martyniuk KM, Chang CY, Abbas AI, Lowes DC, Kellendonk C, Gogos JA, Gordon JA (2021) Reset of hippocampal-prefrontal circuitry facilitates learning. Nature 591:615–619.
- Park J, Moghaddam B (2017) Risk of punishment influences discrete and coordinated encoding of reward-guided actions by prefrontal cortex and VTA neurons. Elife 6.
- Perez-Lopez JL, Contreras-Lopez R, Ramirez-Jarquin JO, Tecuapetla F (2018) Direct glutamatergic signaling from midbrain dopaminergic neurons onto pyramidal prefrontal cortex neurons. Front. Neural Circuits 12:70.
- Quiroga RQ (2012) Spike sorting. Curr. Biol. 22:R45-R46.
- Riaz S, Puveendrakumaran P, Khan D, Yoon S, Hamel L, Ito R (2019) Prelimbic and infralimbic cortical inactivations attenuate contextually driven discriminative responding for reward. Sci. Rep. 9:3982.
- Salvetti B, Morris RG, Wang SH (2014) The role of rewarding and novel events in facilitating memory persistence in a separate spatial memory task. Learn. Mem. 21:61–72.

- Schwartz B, Wasserman EA, Robbins SJ (2002) Psychology of Learning and Behavior, fifth ed. W.W. Norton.
- Shipman ML, Trask S, Bouton ME, Green JT (2018) Inactivation of prelimbic and infralimbic cortex respectively affects minimally-trained and extensively-trained goal-directed actions. Neurobiol. Learn. Mem. 155:164–172.
- Sotres-Bayon F, Sierra-Mercado D, Pardilla-Delgado E, Quirk GJ (2012) Gating of fear in prelimbic cortex by hippocampal and amyodala inputs. Neuron 76:804–812.
- Swindale NV, Mitelut C, Murphy TH, Spacek MA (2017) A visual guide to sorting electrophysiological recordings using 'SpikeSorter'. J. Vis. Exp..
- van Kesteren MT, Ruiter DJ, Fernandez G, Henson RN (2012) How schema and novelty augment memory formation. Trends Neurosci. 35:211–219.
- Wang C, Furlong TM, Stratton PG, Lee CCY, Xu L, Merlin S, Nolan C, Arabzadeh E, Marek R, Sah P (2021) Hippocampus-prefrontal coupling regulates recognition memory for novelty discrimination. J. Neurosci. 41:9617–9632.
- Wu X, Gu X, Guo Q, Hao X, Luo J (2022) Neural correlates of novelty and appropriateness processing in cognitive reappraisal. Biol. Psychol. 170 108318.
- Yoo JH, Zell V, Gutierrez-Reed N, Wu J, Ressler R, Shenasa MA, Johnson AB, Fife KH, Faget L, Hnasko TS (2016) Ventral tegmental area glutamate neurons co-release GABA and promote positive reinforcement. Nat. Commun. 7:13697.
- Zielinski MC, Shin JD, Jadhav SP (2019) Coherent coding of spatial position mediated by theta oscillations in the hippocampus and prefrontal cortex. J. Neurosci. 39:4550–4565.

(Received 15 August 2023, Accepted 15 March 2024) (Available online 20 March 2024)